

**This is an electronic reprint of the original article.
This reprint *may differ* from the original in pagination and typographic detail.**

Author(s): Caputo, Christine; Jennings, Michael; Tuononen, Heikki; Jones, Nathan

Title: Phospha-Fischer Carbenes: Synthesis, Structure, Bonding, and Reactions of Pd(0)- and Pt(0)-Phosphenium Complexes

Year: 2009

Version:

Please cite the original version:

Caputo, C., Jennings, M., Tuononen, H., & Jones, N. (2009). Phospha-Fischer Carbenes: Synthesis, Structure, Bonding, and Reactions of Pd(0)- and Pt(0)-Phosphenium Complexes. *Organometallics*, 28(4), 990-1000.
<https://doi.org/10.1021/om800973v>

All material supplied via JYX is protected by copyright and other intellectual property rights, and duplication or sale of all or part of any of the repository collections is not permitted, except that material may be duplicated by you for your research use or educational purposes in electronic or print form. You must obtain permission for any other use. Electronic or print copies may not be offered, whether for sale or otherwise to anyone who is not an authorised user.

Phospha-Fischer Carbenes: Synthesis, Structure, Bonding and Reactions of Pd(0)– and Pt(0)– Phosphenium Complexes

Christine A. Caputo,^a Michael C. Jennings,^a Heikki M. Tuononen^b and Nathan D.

Jones^{a,}*

^a Department of Chemistry, The University of Western Ontario, London, Ontario, Canada
N6A 5B7. Fax: 1-519-661-3022.

^b Department of Chemistry, University of Jyväskylä, P.O. BOX 35, FI-40014 Jyväskylä,
Finland

Email: njones26@uwo.ca

Abstract

The analogy between cationic Group 10 metal–phosphenium complexes and Fischer carbenes has been formalized through structural and reactivity studies, and by energy decomposition analysis (EDA) of the M–P bond. The studied compounds were the three-coordinate, 16-electron species $[(\text{NHP}^{\text{Mes}})\text{M}(\text{PPh}_3)_2]\text{OTf}$ (M = Pt (**1**) and Pd (**2**); $[\text{NHP}^{\text{Mes}}]^+$ is the *N*-heterocyclic phosphenium (NHP) cation, $[\text{PN}(2,4,6\text{-Me}_3\text{-C}_6\text{H}_2)\text{CH}_2\text{CH}_2\text{N}(2,4,6\text{-Me}_3\text{-C}_6\text{H}_2)]^+$, OTf = trifluoromethanesulfonate); these were made by reaction of $[\text{NHP}^{\text{Mes}}]\text{OTf}$ with $\text{M}(\text{PPh}_3)_4$. The metal–phosphenium bond in both compounds was dominated by metal-to-ligand π -donation. This differed from the M–C bonds in the analogous *N*-heterocyclic carbene (NHC) complexes, $(\text{NHC}^{\text{Mes}})\text{M}(\text{PPh}_3)_2$ (M = Pt (**6**), Pd (**7**)) that were instead predominantly σ -type. Structural determination of **1** by X-ray crystallography revealed the shortest yet reported Pt–P bond of 2.107(3) Å, consistent with significant double bond character, and trigonal planar geometries at both the P-atom within the $[\text{NHP}^{\text{Mes}}]^+$ ligand ($\sum(\text{angles}) = 359.99^\circ$) and at the Pt-atom ($\sum(\text{angles}) = 360.00^\circ$), which indicated that **1** was better described as a Pt(0)–phosphenium rather than as a Pt(II)–phosphide. Reactions of **1** and **2** with excess PMe_3 cleanly gave the four coordinate species, $[(\text{NHP}^{\text{Mes}})\text{M}(\text{PMe}_3)_3]\text{OTf}$ (M = Pt (**3**) and Pd (**4**)), while reaction of **1** with bis(diphenylphosphino)ethane (dppe) gave $[(\text{NHP}^{\text{Mes}})\text{Pt}(\text{dppe-}\kappa^2\text{P})(\text{dppe-}\kappa\text{P})]\text{OTf}$ (**5**). Hydrolysis of these complexes resulted in metal hydrides, and oxidation of the NHP to phosphine oxide *via* initial nucleophilic attack of water at the P-atom in the coordinated $[\text{NHP}^{\text{Mes}}]^+$ ligand, which was calculated to bear a +1.09 charge in **1**.

Introduction

The unfurling of new molecular metal chemistry relies to a great extent on the discovery and development of novel ancillary and reactive ligand types with unusual electronic and steric demands. These initially strange ligands often permit the generation of unfamiliar metal coordination geometries, and the stabilization of unusual oxidation states. They also impart unique reactivity on the resulting complexes, which may in turn lead to significant applications. There are few better examples than that of metal-carbenes, which have revolutionized organometallic chemistry and catalysis. The pioneering work in this area by Fischer,^{1,2} Schrock,^{3,4} Grubbs,⁵ Arduengo⁶ and Bertrand,^{7,8} has been extended to include analogous complexes of the main group elements, *e.g.*, boron (boryls, $:\text{BR}_2^-$),^{9,10} silicon (silylenes, $:\text{SiR}_2$),^{11,12} and phosphorus (phospheniums, $:\text{PR}_2^+$).¹³⁻¹⁷

N-heterocyclic phosphenium cations (NHP) are the “carbon copies” of the now ubiquitous Arduengo-type carbenes (NHC).¹⁸ Both species may have saturated or unsaturated “backbones,” but this report deals only with the saturated variety, specifically the mesityl-substituted compound, $[\text{NHP}^{\text{Mes}}]\text{OTf}$ (Chart 1). The *N*-heterocyclic carbenes and phospheniums are isostructural and isovalent, but electronically inverse. NHC are strong σ -donors and weak π -acceptors, whereas NHP are weak σ -donors and good π -acceptors on account of the formal positive charge and isotropic *s*- (as opposed to directional sp^2 -) character of the “lone pair” orbital on phosphorus.¹⁹ The two families should therefore show reciprocal reactivity in transition metal chemistry.²⁰

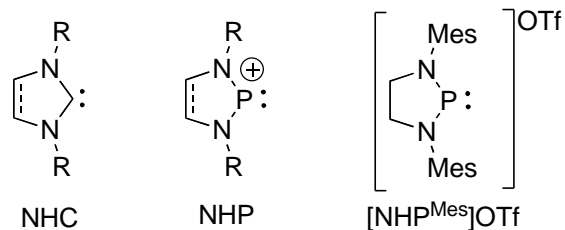


Chart 1. Comparison between *N*-heterocyclic carbenes (NHC) and phospheniums (NHP), and the specific ligand under study, [NHP^{Mes}]OTf (Mes = 2,4,6-trimethylphenyl, TfO⁻ = trifluoromethanesulfonate).

Often considered “phosphine replacement” ligands,²¹⁻²³ NHC have triggered an explosion of research in the field of homogeneous catalysis. By comparison, NHP have garnered much less attention as ancillary ligands in catalysis. However, reinvigorated investigation of their metal chemistry over the last several years has begun to uncover their remarkable properties.^{13,24}

The use of diaminophospheniums as ligands dates to Parry’s 1978 synthesis of [(CO)₄Fe(P{NR₂}₂)]PF₆.²⁵ Since then, the synthesis, structure, bonding and reactivity of early and mid-transition metal complexes (*e.g.*, of Cr,^{26,27} Mo,^{28,29} W,^{26,27} Fe³⁰ and Ru³¹) have been explored, principally by Nakazawa.¹⁴ To date, however, there are exceedingly few reported examples of late (Group 9 and 10) transition metal-NHP complexes. The groups of Baker³² and Richeson²⁰ have both made NHP-containing analogues of Wilkinson’s catalyst (**I–III**; Chart 2) and Gudat has disclosed a Co complex (**IV**).³³ To the best of our knowledge, there are currently only four reported NHP complexes of the Group 10 metals. The first of these was [(NHP^{Mes})Ni(CO)₃][BH^sBu₃] (**V**) by Parry.³⁴ Niecke has described a Ni complex with a zwitterionic phosphonium-containing ligand

(VI),³⁵ while Baker has shown that $[\text{NHP}^{\text{Mes}}]\text{OTf}$ reacts directly with $\text{Pt}(\text{PPh}_3)_3$ to give $[(\text{NHP}^{\text{Mes}})\text{Pt}(\text{PPh}_3)_2]\text{OTf}$ (**1**).³⁶ One of the PPh_3 ligands in this complex can be replaced by an Enders-type NHC to give $[(\text{NHP}^{\text{Mes}})\text{Pt}(\text{PPh}_3)(\text{NHC})]\text{OTf}$ (**VII**); the same compound results from reaction between $\text{Pt}(\text{PPh}_3)_3$ and the $\text{NHC} \rightarrow \text{NHP}$ adduct.

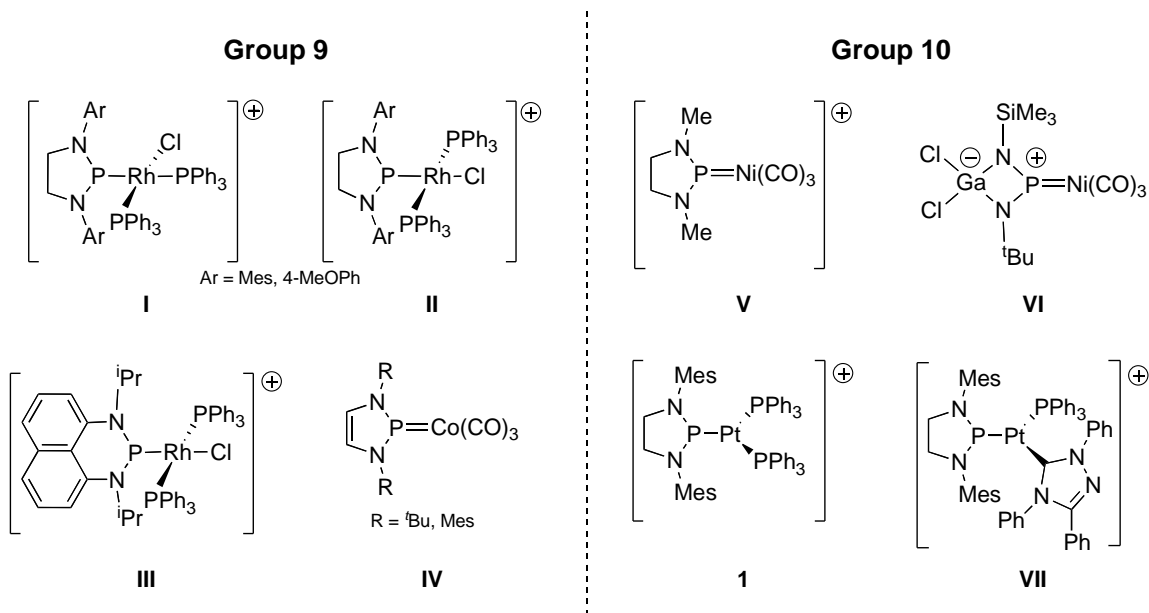


Chart 2. Summary of reported Group 9 and 10 metal-NHP complexes. With the exception of **1** and **VII** for which graphics were not given in the original reports, the cations are drawn exactly as they have been represented in the literature. In all Pt and Rh compounds, the anion is TfO^- ; for Ni, it is $[\text{HB}(\text{sBu})_3]^-$.

Based on their strong π -acidity and reasonably straightforward modular synthesis, NHP have been described as tunable CO equivalents.³² However, it may be better to think of

them as tunable NO^+ surrogates instead, not only because they are cationic but also because, in contrast to terminal CO ligands that bind only linearly, they may in principle adopt either planar or pyramidal (at P) coordination modes.³⁷ These are analogous to the linear and “bent” modes, respectively, of metal nitrosyls, and have identical implications for oxidation state formalisms (Chart 3). The planar ligand is properly considered a coordinated phosphonium, while the pyramidal one is a metal phosphide. Both of these modes have been observed structurally by Paine in $\text{CpMo}(\text{CO})_2(\text{NHP}^{\text{Me}})$ (planar)³⁸ and $\text{Cp}^*\text{Fe}(\text{CO})_2(\text{NHP}^{\text{Me}})$ (pyramidal).³⁹ The analogy between NHP and NO^+ (and Fischer carbenes, *vide infra*) was first drawn in passing in Paine’s pioneering work, and also later in a review by Gudat,¹³ but to the best of our knowledge the relationship has not been formalized *via* definitive structure, bonding and reactivity relationships.

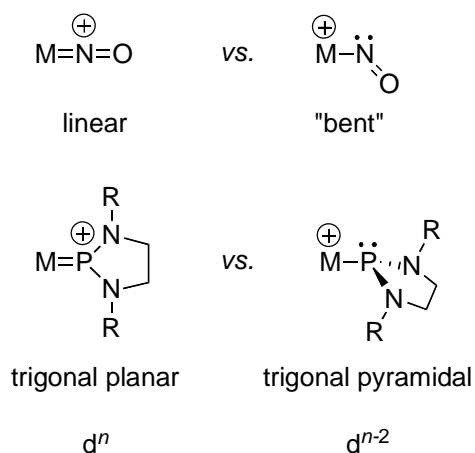


Chart 3. Structural analogy between metal-nitrosyls and -phospheniums.

Just as there is inconsistency in the ways that metal-NHC bonds are drawn in the literature, representation of the metal-NHP interaction has proven problematic (see Chart 2 for the ways that Group 9 and 10 metal complexes have been drawn, and Chart 4 for

various generic representations). Although a range of descriptions is warranted on the basis of differences in structure and reactivity, and therefore a universally applicable drawing is impossible, historical representation of the metal-NHP interaction appears to be complicated by the ligand's carbene-like nature, formal positive charge, dual bonding modes and capacity for strong π -backbonding. The representations in Chart 4 may be considered to be on the same "resonance continuum," sometimes by deconvolution of the dative bond, $D \rightarrow A$, to its charge-separated, valence bond representation, $D^+ - A^-$,⁴⁰ but these diagrams have different chemical *meanings* and should have significant implications in interpreting and predicting the structures and reactivity of the NHP complexes they represent. For example, it should be possible to substitute the phosphonium ligand in **A**; and **B** should contain a trigonal pyramidal phosphorus centre with a lone pair (as in Chart 3), although it has been used in the literature to represent coordinated planar phosphoniums.

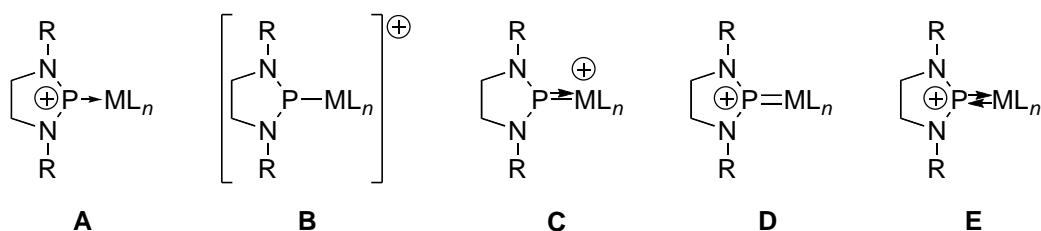


Chart 4. A selection of generic representations of metal-NHP complexes found in the literature.

We recently reported an improved synthesis of a family of free saturated NHP ligands.⁴¹ In this article, we present a series of cationic Pt(0)- and Pd(0)-NHP complexes

(Chart 5, including **1** *via* a new synthesis) followed by their reactions with both monodentate and chelating tertiary phosphines, and also with H₂O.

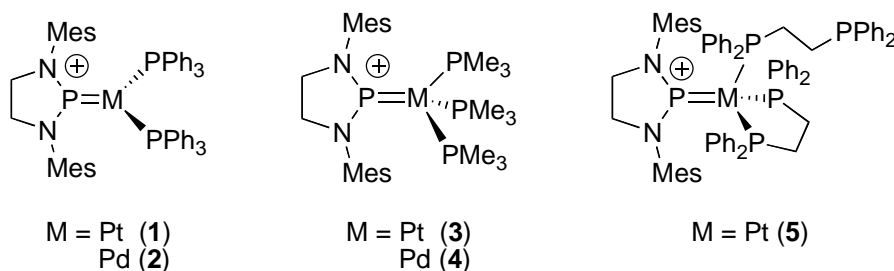


Chart 5. NHP-containing compounds made in this study. All anions are TfO⁻.

The solid state structure of **1** presented herein, together with the results of electronic structure calculations and reactivity patterns afford insight into the nature of the bonding in late metal-NHP complexes and allow the analogy to carbenes and linear nitrosyls to be put on a solid footing. The Pt and Pd compounds are best described as phosphorus analogues of Fischer carbenes with P=M double bond character and localization of positive charge at P (as in **D**, Chart 4). To demonstrate this analogy to Fischer carbenes, we show that the coordinated phosphonium ligand is inert to substitution by monodentate and chelating phosphines. We show also that the complexes undergo attack by H₂O at the NHP P-atom to generate metal-hydrides in a mechanism akin to that proposed for the hydrolysis of Fischer carbenes.⁴²⁻⁴⁴

Experimental Section

General Considerations

Reagents were obtained from commercial sources and used as supplied, unless otherwise indicated. These were of American Chemical Society (ACS) grade or finer. Solvents were dried and deoxygenated either by N₂ purge followed by passage through alumina columns (Innovative Technology or MBraun solvent purification systems), or by distillation under N₂ from the appropriate drying agent. All reactions were carried out under N₂ atmosphere using standard Schlenk techniques unless stated otherwise. Pt(PPh₃)₄ and Pd(PPh₃)₄ were made according to literature procedures.^{45,46}

¹H, ¹³C{¹H}, ¹⁹F{¹H}, ³¹P{¹H} NMR data were recorded on 400 MHz Varian Mercury (400.085 MHz for ¹H, 100.602 MHz for ¹³C, 376.458 MHz for ¹⁹F) or 400 MHz Varian Inova spectrometer (399.762 MHz for ¹H, 100.520 MHz for ¹³C, 161.825 MHz for ³¹P). Unless otherwise indicated, spectra were recorded at r.t. in CDCl₃ solution using residual solvent proton (relative to external SiMe₄, δ 0.00) or solvent carbon (relative to external SiMe₄, δ 0.00) as an internal reference. All ³¹P{¹H} NMR spectra were recorded relative to an external standard (85 % H₃PO₄, δ 0.00). Downfield shifts were taken as positive, and all coupling constants are given in Hertz.

High resolution mass spectrometry data were recorded using a Finnigan MAT 8200 instrument. Elemental analyses (C, H, N) were performed by Guelph Chemical Laboratories Inc., Guelph, ON, Canada.

Synthesis of Pt and Pd Metal Complexes

[(NHP^{Mes})Pt(PPh₃)₂]OTf (1). The synthesis of this compound (previously reported by Baker and co-workers)³⁶ was modified to use Pt(PPh₃)₄ instead of Pt(PPh₃)₃. In a small vial, Pt(PPh₃)₄ (0.53 g, 0.42 mmol) was dissolved in C₆H₆ (10 mL). A solution of [NHP^{Mes}]OTf (0.20 g, 0.42 mmol) in C₆H₆ (5 mL) was added dropwise to give a dark yellow solution. The solvent was frozen and removed *in vacuo* to give a yellow solid, which was washed with Et₂O (2 × 10 mL) to remove free PPh₃, then dried *in vacuo* to give the title compound as a yellow solid. Yield: 0.26 g (49 %). X-ray quality crystals of 1·½ C₆H₆ were grown from concentrated C₆H₆ solution by slow evaporation. The ¹H NMR spectroscopic data were identical to those reported by Baker.³⁶ However, chemical shift differences due to solvent were observed in the ³¹P{¹H} NMR spectrum. ³¹P{¹H} NMR (CDCl₃): δ 44.3 (d, ¹J_{Pt} = 4243, ²J_{PP} = 228), 290.0 (t, ¹J_{Pt} = 6446, ²J_{P-P} = 228). In addition, the following additional characterization data were collected: ¹⁹F{¹H} NMR (CDCl₃): δ -78.1 (s); ESI-MS: C₅₆H₅₆N₂P₃Pt⁺ calcd (found) 1044.3299 (1044.3367, M⁺). Anal. calcd for C₅₇H₅₈F₃N₂O₃P₃PtS: C, 57.2; H, 4.9; N, 2.3 %. Found: C, 57.2; H, 5.0; N, 2.2 %.

[(NHP^{Mes})Pd(PPh₃)₂]OTf (2). This compound was made in the same way as **1**. Thus, reaction of Pd(PPh₃)₄ (0.59 g, 0.52 mmol) and [NHP^{Mes}]OTf (0.27 g, 0.57 mmol) gave 0.30 g (52 %) of a yellow solid. ¹H NMR (C₆D₆): δ 2.05 (s, 6H, *p*-CH₃), 2.08 (s, 12H, *o*-CH₃), 4.10 (d, 4H, CH₂, ³J_{HP} = 4.0), 6.54 (s, 4H, Ar), 7.01 (pt, 18H, Ar), 7.13 (pq, 12H, Ar). ¹³C{¹H} NMR (CDCl₃, 263 K): δ 17.8, 21.3, 52.5, 128.8, 130.0, 130.3, 131.8, 133.3, 135.0, 136.0, 138.8. ³¹P{¹H} NMR (CDCl₃): δ 25.1 (d, ²J_{PP} = 149), 260.0 (t, ²J_{PP} = 149). ¹⁹F NMR (CDCl₃): δ -78.2 (s). ESI-MS: C₅₆H₅₆N₂P₃Pd⁺ calcd (found) 955.3 (955.3, M⁺).

Anal. calcd for C₅₇H₅₆F₃N₂O₃P₃PdS: C, 61.9; H, 5.1; N, 2.5 %. Found: C, 62.0; H, 5.1; N, 2.5%.

[(NHP^{Me})Pt(PMe₃)₃] (3). Neat PMe₃ (0.25 mL, 2.4 mmol) was added dropwise to a yellow CH₂Cl₂ (2 mL) solution containing **1** (0.33 g, 0.28 mmol) in a small vial. The reaction mixture was stirred for 10 min at r.t. during which it turned red. The solvent was removed *in vacuo*, and the orange residue was washed with Et₂O (2 × 10 mL) to remove free PPh₃ then dried under vacuum. Yield: 0.22 g (88 %). ¹H NMR (CDCl₃): δ 1.17 (m (br m, 27H, CH₃), 2.25 (s, 6H, *p*-CH₃), 2.34 (s, 12H, *o*-CH₃), 3.79 (d, 4H, CH₂, ³J_{HP} = 2.0), 7.28 (br s, 4H, *m*-CH). ¹³C{¹H} NMR (CDCl₃, 273 K): δ 18.7, 21.0, 24.6, 50.7, 129.9, 134.3, 136.6, 138.6. ³¹P{¹H} NMR (CDCl₃): δ -47.1 (d, ¹J_{Pt} = 3283, ²J_{PP} = 125), 207.6 (q, ¹J_{Pt} = 6162, ²J_{PP} = 125). ¹⁹F NMR (CDCl₃): δ -78.1 (s). ESI-MS: C₂₉H₅₃N₂P₄Pt⁺ calcd (found) 748.2807 (748.2743, M⁺). Anal. calcd for C₃₀H₅₃F₃N₂O₃P₄PtS: C, 40.1 H, 5.95; N, 3.1 %. Found: C, 39.65; H, 6.1; N, 2.6 %.

[(NHP^{Me})Pd(PMe₃)₃]OTf (4). This compound was made in the same way as **3**. Thus reaction of **2** (0.30 g, 0.27 mmol) and PMe₃ (0.112 mL, 1.09 mmol) gave 0.13 g (58 %) of an orange solid. ¹H NMR (CDCl₃): δ 1.03 (br s, 27H, CH₃), 2.24 (s, 6H, *p*-CH₃), 2.34 (s, 12H, *o*-CH₃), 3.86 (d, 4H, CH₂, ³J_{HP} = 4.4), 6.95 (s, 4H, Ar). ¹³C{¹H} NMR (CDCl₃): δ 18.7, 21.2, 21.4, 52.1 (d, ²J_{P-C} = 6.1), 128.6 (d, ²J_{P-C} = 7.6), 130.3, 133.8 (d, ²J_{P-C} = 17.7), 134.3 (d, ²J_{CP} = 9.2), 136.3 (d, ²J_{CP} = 3.1), 139.0. ³¹P{¹H} NMR (CDCl₃, 253 K): δ -29.6 (d, ²J_{PP} = 73), 242.8 (d, ²J_{PP} = 73). ¹⁹F NMR (CDCl₃): δ -74.2 (s). ESI-MS: C₂₉H₅₃N₂P₄Pd⁺ calcd (found) 585.2 (583.1, M⁺ - PMe₃), (507.1, M⁺ - 2 PMe₃). Anal. calcd for C₃₀H₅₃F₃N₂O₃P₄PdS: C, 44.53 H, 6.60; N, 3.46 %. Found: C, 44.25; H, 6.52; N, 3.16 %.

[(NHP^{Mes})Pt(dppe- κ^2P)(dppe- κP)]OTf (5). This compound was prepared in the same way as **3**. Thus, reaction of **1** (102 mg, 85.0 mmol) and dppe (68.0 mg, 17.0 mmol) gave 94.7 mg (76 %) of a dark orange solid. ¹H NMR (CDCl₃): δ 1.26 (br s, 4H, PCH₂), 1.58 (br s, 4H, PCH₂), 2.10 (s, 6H, *p*-CH₃), 2.26 (s, 12H, *o*-CH₃), 3.94 (br s, 4H, NCH₂), 6.59 (br s, 4H, Ar), 6.93-7.25 (br m, 40H, Ar). ³¹P{¹H} NMR (CDCl₃, 263 K): δ -14.2 (d, ³J_{PP} = 28.5), 9.7 (m, ¹J_{PPt} = 3502), 26.3 (m, ¹J_{PPt} = 2994, ²J_{PP} = 105), 217.5 (m, ¹J_{PPt} = 6914). ¹⁹F NMR (CDCl₃): δ -78.0 (s). ESI-MS: C₇₂H₇₇N₂P₅Pt⁺ calcd (found) 1319.4 (1320.4, M⁺ +1), (921.9, M⁺ - dppe). The inevitable appearance of [PtH(dppe)₂]OTf hydrolysis product in all samples precluded satisfactory elemental analysis.

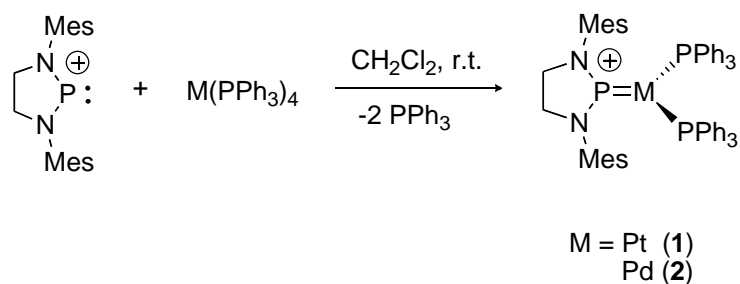
Computational details

Molecular geometries of all studied compounds were optimized with DFT using the GGA PBE/PBE exchange-correlation functional⁴⁷⁻⁴⁹ with the def-TZVP basis sets;^{50,51} ECP basis sets of similar valence quality were used for the transition metal nuclei.⁵² Though the use of GGA functional leads to slight overestimation of all bond lengths, it was preferred over the hybrid counterpart PBE1PBE for reasons of computational efficiency, *i.e.*, the ability to use multipole accelerated RI approximation and to run calculations in parallel. All optimizations were carried out with the Turbomole 5.10 program package.^{53,54} Energy decomposition analyses for optimized structures were performed with the ADF 2007.01 program.⁵⁵ The analysis followed the Morokuma-Rauk-Ziegler partition scheme⁵⁶⁻⁵⁸ and utilized the PBE/PBE GGA functional⁴⁷⁻⁴⁹ in combination with STO-type all-electron basis sets of TZP quality.^{59,60} Scalar relativistic

effects were taken into account in all EDA calculations by employing the ZORA Hamiltonian.⁶¹⁻⁶³ Representations of the molecular orbitals of **2** and **7** given in Figure 2 were constructed using the gOpenMol program.^{64,65}

Results and Discussion

Synthesis and Structure. The phosphonium triflate $[\text{NHP}^{\text{Mes}}]\text{OTf}$ reacts quickly and cleanly with equimolar $\text{M}(\text{PPh}_3)_4$ precursors at r.t. to generate $[(\text{NHP}^{\text{Mes}})\text{M}(\text{PPh}_3)_2]\text{OTf}$ (**1**: $\text{M} = \text{Pt}$; **2**: $\text{M} = \text{Pd}$) with elimination of 2 equiv. of PPh_3 (Scheme 1). As mentioned in the introduction, **1** has previously been made (although not structurally characterized) by reaction of $[\text{NHP}^{\text{Mes}}]\text{OTf}$ with $\text{Pt}(\text{PPh}_3)_3$; **2** represents the first well defined Pd–NHP complex, although related species have been assumed to form *in situ* in catalytic processes.^{66,67}



Scheme 1. Synthesis of Pd(0) and Pt(0)–NHP metal complexes. Anion is TfO^- .

The geometries of mixed phosphine–phosphenium complexes of the type $[(\text{NHP}^{\text{Mes}})\text{M}(\text{PR}_3)_n]\text{OTf}$ are easily elucidated from $^{31}\text{P}\{^1\text{H}\}$ NMR data. The spectrum of **1** in CDCl_3 exhibits an upfield doublet (with Pt satellites) for the PPh_3 ligands (δ 44.3, $^1J_{\text{PtP}} = 4143$ Hz, $^2J_{\text{PP}} = 228$ Hz) and a dramatically downfield triplet (with Pt satellites) for

the coordinated $[\text{NHP}^{\text{Mes}}]^+$ ligand (δ 290.0, $^1J_{\text{PtP}} = 6446$ Hz, $^2J_{\text{PP}} = 228$ Hz) with relative 2:1 peak intensity. These data are similar to those reported by Baker for **1** in CD_2Cl_2 solution.³⁶ They unequivocally confirm the presence of two equivalent phosphine and one phosphonium ligand in a trigonal planar coordination environment. The shift on coordination ($\Delta\delta$) of $[\text{NHP}^{\text{Mes}}]^+$ to Pt is 86.9 ppm downfield, which implies a dramatic deshielding of the phosphorus centre. The Pt-P coupling constant is very much larger than those obtained by Glueck and coworkers⁶⁸ for a range of Pt(II)-phosphide complexes (*ca.* 900–1000 Hz), which implies that the bound NHP in **1** is probably not pyramidal in solution. Similar NMR data are obtained for **2**: an upfield doublet (δ 25.1, $^2J_{\text{PP}} = 149$ Hz) for the PPh_3 ligands and a downfield triplet (δ 260.0, $^2J_{\text{PP}} = 149$ Hz; $\Delta\delta = 56.9$) for the coordinated NHP in a 2:1 ratio show that **1** and **2** are isostructural (Figure 1).

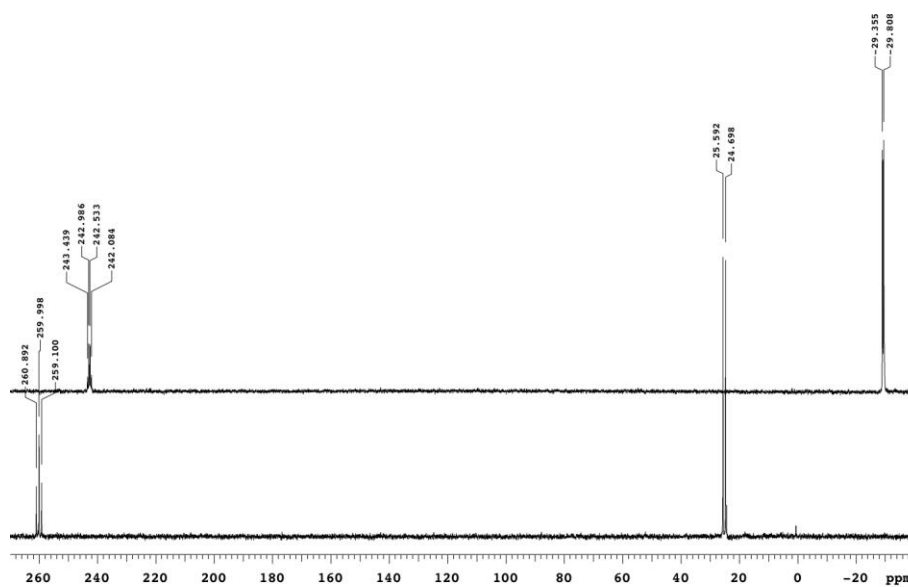


Figure 1. Stacked $^{31}\text{P}\{^1\text{H}\}$ NMR spectra for $[(\text{NHP}^{\text{Mes}})\text{Pd}(\text{PPh}_3)_2]\text{OTf}$ (**2**, bottom) and $[(\text{NHP}^{\text{Mes}})\text{Pd}(\text{PMe}_3)_3]\text{OTf}$ (**4**).

Crystals of $1 \cdot \frac{1}{2} \text{C}_6\text{H}_6$ suitable for X-ray crystallographic analysis were grown at r.t. by slow evaporation of C_6H_6 solution; the solid-state structure is given in Figure 2. As expected from the NMR data, the structure is trigonal planar at Pt ($\Sigma(\text{angles}) = 360.00^\circ$). The geometry at the phosphonium P-atom is also trigonal planar ($\Sigma(\text{angles}) = 359.99^\circ$). The N–P–N plane of the $[\text{NHP}^{\text{Mes}}]^+$ ligand makes a torsion angle of approximately 62° with the coordination plane of the metal. The Pt–NHP bond (Pt–P1: 2.107(3) Å) is significantly shorter than the Pt–PPh₃ bonds (Pt–P2: 2.3178(9) Å and Pt–P3: 2.3113(8) Å) by *ca.* 0.21 Å, consistent with the large Pt–P coupling constant, and indicates a strong Pt–P bond and greater backbonding to the phosphonium than to the PPh₃ ligands. To the best of our knowledge, this Pt–P bond is the shortest reported to date; the previous record of 2.116(3) Å was held by Baker’s complex, **VII** (Chart 2);³⁶ formal Pt=P double bonds in phosphinidenes lie in the range of 2.2 – 2.3 Å,⁶⁹ which contains the average Pt–PPh₃ single bond of 2.28 Å.⁷⁰ These data imply that by metrical considerations alone, the Pt–NHP interaction in **1** may be thought of as a double bond. No short contacts between either the NHP P-atom or the Pt-atom and the TfO[−] anion are observed in the solid state; the closest distances are 3.282 and 3.370 Å between C3 and the OTf[−] O-atoms.

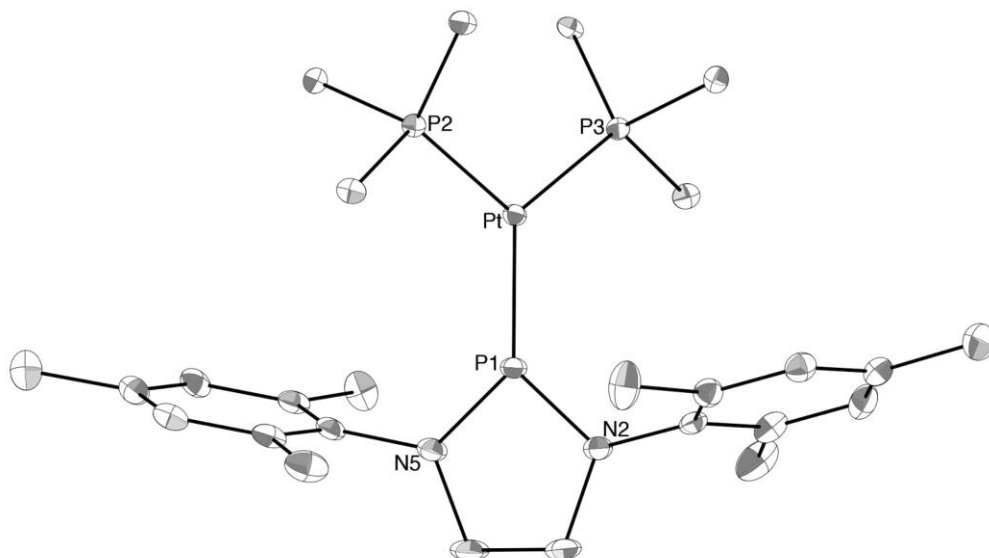


Figure 2. ORTEP representation of the molecular structure of the cation of **1**. Thermal ellipsoids are drawn at 30% probability. H-atoms, TfO⁻ counterion and all but the *ipso*-C-atoms of the PPh₃ ligands have been omitted for clarity. Selected experimental [and calculated] bond distances (Å) and angles (°): Pt–P1, 2.1073(9) [2.185]; P1–N2, 1.640(3) [1.695]; P1–N5, 1.628(3) [1.695]; Pt–P2, 2.3178(9) [2.383]; Pt–P3, 2.3113(8) [2.383]; N5–P1–N2, 93.68(16) [92.0]; N5–P1–Pt, 134.15(12) [134.0]; N2–P1–Pt, 132.16(12) [134.0]; P1–Pt–P3, 121.41(3) [122.0]; P1–Pt–P2, 121.70(3) [122.0]; P2–Pt–P3, 116.89(3) [115.9]; P2–Pt–P1–N5, -61.66(19) [-69.1]; P3–Pt–P1–N5, 119.02(19) [110.9].

The question arises whether to consider **1** as a Pt(0)–NHP complex or a Pt(II)–phosphide (Chart 3). In **1**, and all other structurally characterized Group 9 and 10 metal–NHP complexes,^{20,32,35,36} the geometry at the NHP P-atom is trigonal planar, which clearly rules out the Pt(II)–phosphide description (analogous to “bent” metal–nitrosyls) and thereby discounts formal two-electron oxidation of the metal by the phosphonium.

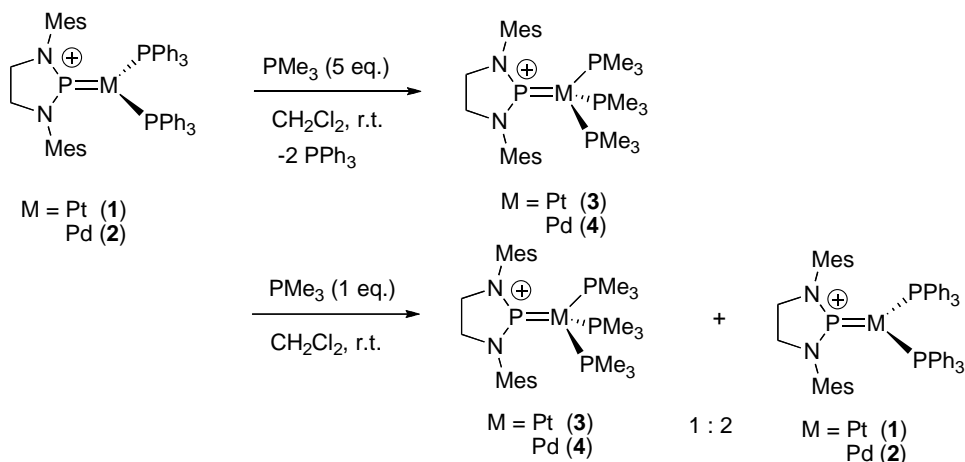
Hence, structural characteristics alone imply that **1** and **2** are best described as 16-electron metal(0)–NHP complexes.

Although **1** should be considered as a compound of Pt(0), it reacts differently from homoleptic Pt(0)–phosphine complexes: it does not dissociate phosphine in solution (within the limits of ^{31}P NMR detection); it is inert to oxidative addition by MeI and MeOTf; and it does not bind the electron-poor alkene, dimethylmaleate. These findings indicate that **1** is significantly less electron rich than other Group 10 metal(0) phosphine compounds, probably on account of the formal positive charge borne by the NHP ligand.

Chart 4 shows a selection of generic representations of metal–NHP complexes found in the literature. Clearly, **B** is not a good description of either **1** or **2** because it implies a trigonal pyramidal geometry at the NHP P-atom. Representation of the M–NHP interaction in **1** and **2** as **D** (equivalent to **E**) should mean (*i*) that the NHP is not easily substituted (the opposite of what would be predicted by **A**), and (*ii*) that the ligand should suffer attack by good nucleophiles; representation instead as **C** would predict attack by nucleophiles at the metal rather than the phosphorus centre. In fact, both predictions (*i*) and (*ii*) are borne out by experiment.

To test the first hypothesis, we surveyed the reaction of **1** and **2** with a variety of monodentate and chelating phosphines, and in no case was the NHP ligand displaced from the inner coordination sphere of the metal. This finding is consistent with Baker's observation that reaction of **1** with an NHC leads to the mixed NHP/NHC compound **VII** in which the phosphonium ligand is retained.³⁶ In our study, reaction of **1** and **2** with an excess of the small, basic phosphine PMe_3 quickly and cleanly gives $[(\text{NHP}^{\text{Mes}})\text{M}(\text{PMe}_3)_3]\text{OTf}$ (**3**: M = Pt; **4**: M = Pd). The substitution of PPh_3 by PMe_3 is cooperative, so that when only a single equivalent of PMe_3 is added, **3** and **4** are

generated, but 2/3 of the starting material is present in the reaction mixture at completion (Scheme 2). In no case is a mixed $\text{PMe}_3/\text{PPh}_3$ complex detected, and the NHP ligand is always retained.

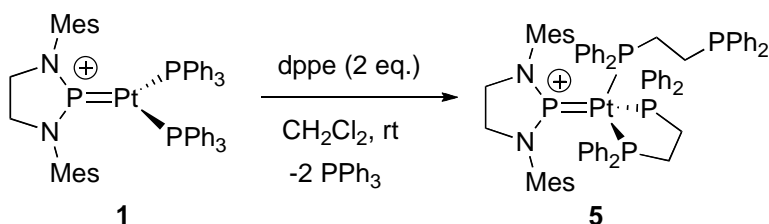


Scheme 2. Phosphine substitution reactions of **1** and **2** with PMe_3 . All anions are TfO^- .

The formation of four- rather than the three-coordinate products could be explained by the smaller steric demand of PMe_3 compared to PPh_3 (Tolman cone angles: 118° and 143° , respectively)⁷¹ and also to the higher Lewis basicity of the incoming ligand. The $^{31}\text{P}\{^1\text{H}\}$ NMR spectroscopic data of **3** and **4** are similar to those of the parent compounds, except that in these cases the downfield peaks due to the coordinated NHP are quartets, rather than triplets, due to coupling of the NHP to three equivalent phosphines in the four-coordinate products (Figure 1). These complexes are best described as 18-electron metal(0)–NHP complexes. Putative metal(II) compounds bearing three phosphine ligands should be square planar and therefore have two chemically distinct PR_3 environments, one *trans* to the NHP and the other *cis*. However, in **3** and **4** only a single PMe_3 environment is evident by NMR spectroscopy, which indicates the presence of the three

equivalent phosphine ligands in a tetrahedral complex, and thereby reinforces the idea that these compounds (together with **1** and **2**) are in fact metal(0) species.

Reaction of **1** with the chelating phosphine, bis(diphenylphosphino)ethane (dppe), gives **5** with substitution of both PPh₃ ligands (Scheme 3). This compound has a distinctive ³¹P{¹H} NMR spectrum that unequivocally describes the structure. The spectrum of **5** displays a low field multiplet (with Pt “satellites”) at τ^M 215.6, an upfield multiplet (τ^M 26.4, showing Pt “satellites”), yet another multiplet in this region (τ^M 9.73, showing Pt “satellites”), and a doublet even further upfield (τ^M -14.2, no coupling to Pt). The chemical shifts, multiplicities and relative integrations of these four chemically inequivalent ³¹P environments are consistent with the presence of coordinated [NHP^{Mes}]⁺, and one chelating and one monodentate dppe ligand, *i.e.*, the compound [(NHP^{Mes})Pt(dppe-²P)(dppe-¹P)]OTf (Scheme 3). This once again is clear evidence of the substitutionally inert nature of the coordinated NHP, and reinforces the notion that **1** is properly considered as a phospha-Fischer carbene.



Scheme 3. Substitution reactions of **1** with dppe. Anion is TfO⁻.

Bonding. The qualitative bonding scheme describing cyclic aminophosphenium ions as σ -donors and π -acceptors emerged concurrently with the publication of the first X-ray

crystal structures of NHP-metal complexes.³⁸ By contrast, quantitative treatments of the M–P bond in these systems are rare and vastly outnumbered by analyses of the M–C interaction in metal–NHC complexes, which have been intensely scrutinized using a myriad of computational approaches.⁷²⁻⁷⁸ The most authoritative investigations into M–NHP bonding have been published by Gudat and coworkers.^{24,33,79} Together with others in the field,⁸⁰ they have analyzed the M–P bond primarily with orbital-based approaches, such as Mulliken and natural population analyses. To the best of our knowledge, there are no reports of an energy decomposition analysis (EDA) of M–NHP bonding within the framework of a fragment molecular orbital (FMO) approach.⁵⁶⁻⁵⁸ This combination of methods is aptly suited for the analysis of donor-acceptor interactions because it allows a simple quantification of the relative importance of σ - and π -contributions to bonding.

The EDA approach has been extensively described in the literature⁸¹ and only a brief overview is presented herein. The energy associated with bond formation between two (or more) fragments – typically the metal and the ligand(s) – both possessing the geometry they take in the optimised complex, is referred to as the total bonding energy ΔE_{tot} .⁸² According to EDA, ΔE_{tot} can be expressed as a sum of steric, ΔE^0 , and orbital, ΔE_{orbint} , interactions, *i.e.*, $\Delta E_{\text{tot}} = \Delta E^0 + \Delta E_{\text{orbint}}$. The steric interaction consists of a purely electrostatic term, ΔE_{elstat} , and a Pauli repulsion term, ΔE^{Pauli} , between occupied orbitals on both fragments. The former stabilizes the bond, while the latter weakens it. It is the relative importance of the two terms that determines the effect of ΔE^0 on the total bonding energy. The orbital interaction energy has a stabilizing contribution and is calculated as the energy gain resulting from the relaxation of the FMOs to their optimal form in the complex. This term has an instructive interpretation as a sum of contributions from the various irreducible representations of the molecular point group. Therefore, by

assessing the symmetry of the system, the σ - and π -characteristics of the interaction can be determined in a straightforward manner.

We have examined the bonding in complexes **1–4** using the EDA method. Because the M–P bond is the interaction of interest, the complexes were divided to two parts: the $[\text{NHP}^{\text{Mes}}]^+$ ligand, and the formally 14- and 16-electron fragments $\text{M}(\text{PPh}_3)_2$ and $\text{M}(\text{PMe}_3)_3$, respectively ($\text{M} = \text{Pd}, \text{Pt}$). Analogous valence isoelectronic complexes involving the neutral NHC^{Mes} ligand (**6–9**, Chart 6) were included in the analysis for comparative purposes; the results can also be contrasted to those published earlier for a variety of Fischer carbenes.^{75,83,84}

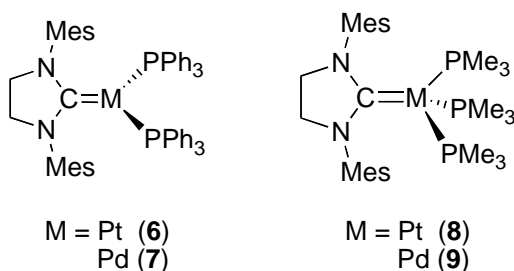


Chart 6. Theoretical Pt and Pd NHC complexes, with M=C bonds drawn analogously to the M=P bonds of **1–4**.

The geometries of all systems were fully optimized prior to EDA calculations. Selected calculated metrical parameters for **1** are given in the legend for Figure 2, and complete structural data are deposited as Supporting Information (SI). The calculated geometries are in good overall agreement with the experimental data and display all the expected trends; therefore an in-depth analysis of geometrical parameters is not warranted. However, special attention should be drawn to three points (*i*) The M–P bond lengths in

1–4 are not significantly affected by the identity of the metal fragment, and indicate multiple bonding in all compounds (the calculated bond lengths lie in the range 2.179–2.199 Å). In contrast, the calculated M–C bond lengths in the analogous NHC complexes **6–9** vary more widely (from 2.050 to 2.145 Å) and are slightly longer than typical measured NHC-Pt(0) and NHC-Pd(0) single bonds in two coordinate complexes (2.02 – 2.09⁸⁵ and 1.99 – 2.11 Å, respectively).⁸⁶⁻⁹⁰ (ii) The geometry at the P- and C-atoms of **1–4** and **6–9**, respectively, is invariably trigonal planar with the sum of bond angles being very close to 360°. (iii) The optimized geometries of **3** and **4** are tetrahedral at the metal center, in agreement with the NMR data.

Results of the EDA calculations are summarized in Table 1. They show that changing the metal from Pd to Pt strengthens the M–P bond by *ca.* 60 kJ mol⁻¹; a change in the composition of the metal fragment from M(PPh₃)₂ to M(PMe₃)₃ further strengthens the bond by 40 kJ mol⁻¹. The overall effect of steric interaction in **1–4** is destabilizing, unlike the case of Fischer carbenes,^{75,83,84} because of the increased Pauli repulsion. However, the total orbital interaction, which is the more informative of the two contributors to ΔE_{tot} , outweighs the steric term for all systems. Furthermore, the C₂-symmetry of **1** and **2** allows us to describe the M–P bond by clean deconvolution of ΔE_{orbint} in these complexes into σ - and π -MOs, which belong to the irreducible representations *a* and *b* of the C₂ point group, respectively⁹¹ (Table 1). This treatment reveals that the bond has approximately 2/3 π - and 1/3 σ -character. Though the same analysis cannot be conducted for the tetrahedral compounds **3** and **4**, we note that their similarity to **1** and **2** in terms of other bonding characteristics (Table 1), together with the FMO analysis (*vide infra*), imply predominant π -bonding also in these complexes.

Table 1. Results of energy decomposition analyses (kJ mol⁻¹) of **1–4** and **6–9**.

	ΔE_{tot}	ΔE^0	ΔE_{elstat}	ΔE^{Pauli}	ΔE_{orbint}	
					<i>a</i>	<i>b</i>
1	-318.5	195.5	-641.9	837.3	-191.0 (37%)	-323.0 (63%)
2	-265.1	138.8	-496.5	635.2	-133.2 (33%)	-270.7 (67%)
3	-359.0	175.9	-644.3	820.2	-534.9	
4	-293.2	136.7	-506.6	643.2	-429.9	
6	-226.3	121.5	-803.8	925.3	-230.2 (66%)	-117.5 (34%)
7	-157.4	67.2	-555.7	622.8	-140.4 (63%)	-84.2 (37%)
8	-191.1	114.9	-718.0	832.8	-305.9	
9	-126.9	68.2	-495.1	563.3	-195.1	

These findings are in stark contrast to those of NHC complexes **6–9**. Though carbenes have long been considered pure σ -donors, recent computational treatments have demonstrated a small to moderate (10 – 30 %) π -bonding character, the significance of which increased with the increasing formal d-electron count.^{75,76,92} Energy decomposition analysis for **6–9** yielded similar π -bonding contributions of 37 and 34 % for **7** and **6**, respectively. For Fischer carbenes, the percentage of ΔE_{orbint} attributable to π -bonding has been reported to lie between 25 and 50 %.^{75,83,84} Therefore, the bonding in **1–4** is clearly of Fischer type also at the quantitative level and, as anticipated,⁷⁹ the M–NHP bond is dominated by π -backbonding.

The bonding in Fischer carbenes and M–NHC complexes can be explained qualitatively by dative and retrodative components whose relative contributions lead to formal double and single M–C bonds in the former and latter species, respectively.^{93,94}

That is, in both cases there generally exists one σ -type MO that is a linear combination of occupied ligand-based orbitals (typically the highest occupied FMO) and unoccupied metal-based d-orbitals, and one π -type MO that is a linear combination of unoccupied ligand-based orbitals (typically the lowest unoccupied FMO) and occupied metal-based d-orbitals. The MOs of **1** and **2** differ significantly from the above classical description, however, and reflect the dominant nature of the π -interaction. Figure 3 illustrates this difference by comparing the important bonding MOs of **2** and **7**. In the NHP complexes **1** and **2**, the unoccupied metal-based d-orbitals make only a negligible to small contribution to the HOMOs of the resultant complexes (6.8 and 0.0 %), whereas the σ -bonding MOs of the NHC complexes **6** and **7**, contain 12.8 and 6.0 % contributions, respectively, from the unoccupied metal-based d-orbitals. By contrast, there is a much greater mixing between the occupied metal-based d-orbitals and the lowest unoccupied FMO of the $[\text{NHP}^{\text{Mes}}]^+$ fragment: this ligand-based FMO contributes 18.8 and 15.3 % to the HOMOs of **1** and **2**, respectively. The analogous contributions to the π -bonding MOs of complexes **6** and **7** are only 8.3 and 5.2 %, respectively. There is also a third bonding contribution in **1** and **2** that is absent from the analogous NHC complexes: due to the cationic charge borne by the $[\text{NHP}^{\text{Mes}}]^+$ fragment, the π -symmetric LUMO+1 of the ligand is also sufficiently low in energy to accept electron density from the occupied metal-based d-orbitals. This results in a second backbonding contribution that is, however, of lesser importance than the primary π -interaction; the percentage contribution of LUMO+1 to the bonding MOs of the metal complex are 6.0 and 5.1 % in **1** and **2**, respectively.

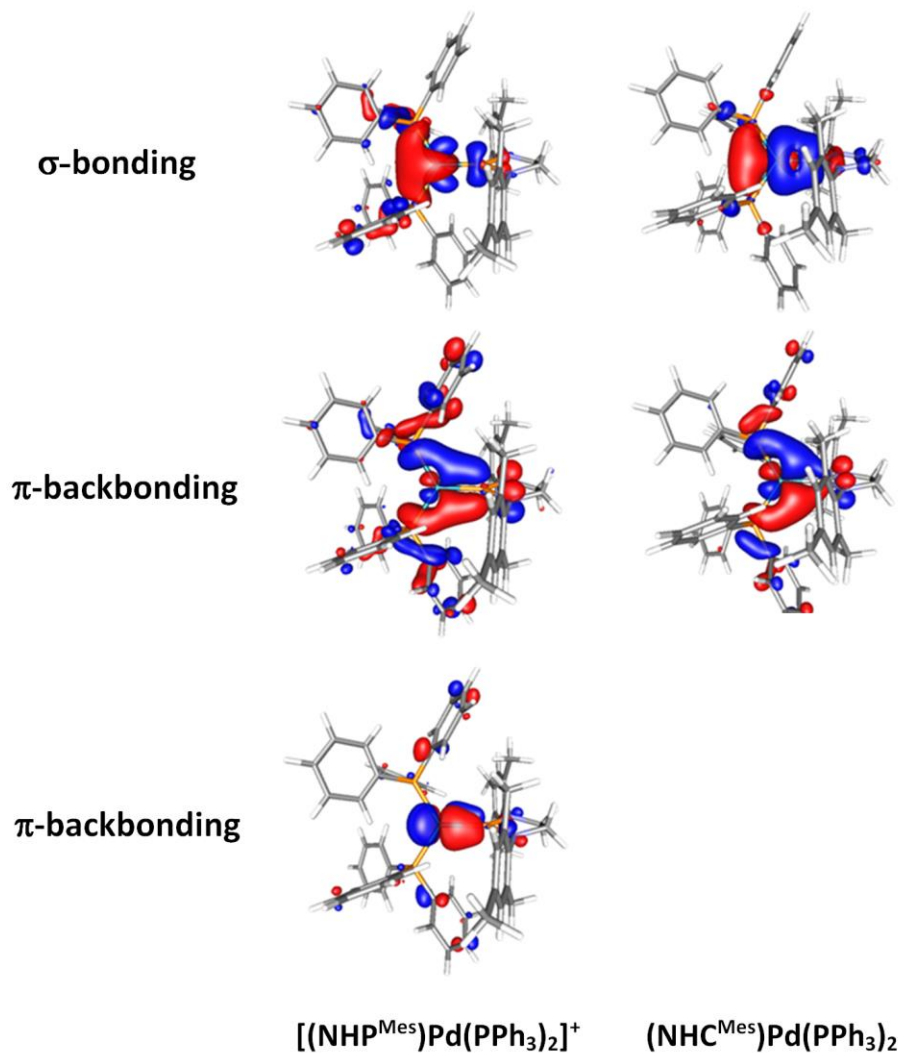
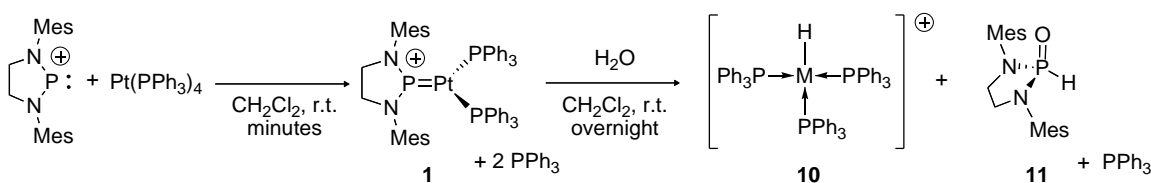


Figure 3. Important bonding MOs in $[(\text{NHP}^{\text{Mes}})\text{Pd}(\text{PPh}_3)_2]^+$ (**2**) and $(\text{NHC}^{\text{Mes}})\text{Pd}(\text{PPh}_3)_2$ (**7**). In all cases the coordination plane of the metal is oriented parallel to the page.

The qualitative bonding description of **3** and **4** (as well that of **8** and **9**) closely follows the above discussion. The most notable difference is the increased importance of the σ -type dative interaction: the unoccupied metal-based d-orbitals have 8.0 and 4.4 % contributions to the occupied MOs of the resulting complexes **3** and **4**, respectively. Even

so, the retrodonative π -interaction dominates the bonding in both compounds. It can therefore be concluded that the net flow of electrons in **1–4** takes place from metal to ligand, but, as evidenced by the calculated data, the transfer of electrons involves significantly less than an electron pair. Thus, the NHP complexes can be considered containing the metal center in a formal zero oxidation state.

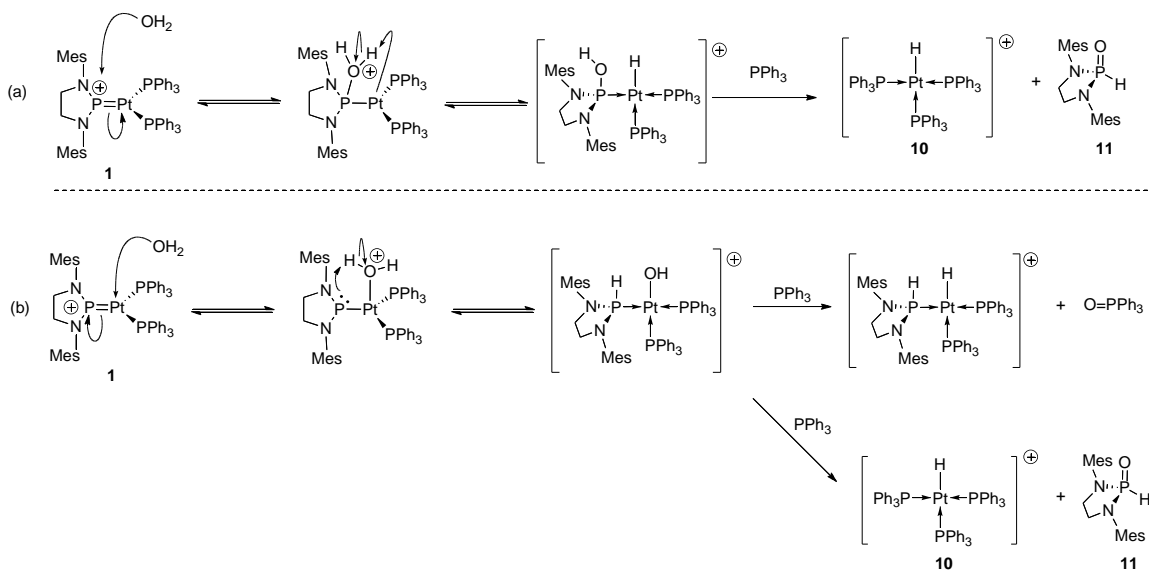
Hydrolysis. Serendipitous discovery of the reaction between **1** and H₂O confirmed the second of the two hypotheses given above, *i.e.*, that these phospho-Fischer carbenes should be susceptible to attack by nucleophiles. Indeed, **1** is highly sensitive to moisture and needs to be handled under rigorously inert atmosphere. Despite repeated drying of solvents, the presence of adventitious water eventually leads to the decomposition of these complexes. Overnight incubation of reaction mixtures of [NHP^{Mes}]OTf and Pt(PPh₃)₄ in wet CH₂Cl₂ or CDCl₃ solution invariably gives a mixture of the well-known Pt(II)-hydride, [PtH(PPh₃)₃]OTf (**10**)⁹⁵⁻⁹⁸ and the phosphine oxide, **11**, which has been independently characterized by Ackermann and Born (Scheme 4).⁶⁶



Scheme 4. Complete *in situ* hydrolysis of **1** in wet CH₂Cl₂ solution. Anion is TfO⁻.

Hydrolysis of **1** may reasonably occur *via* one of two routes, both of which formally involve hydration of the Pt=P double bond, but are differentiated by the regiochemistry of addition: Scheme 5(a) – Initial attack of H₂O at the NHP, followed by protonation of the Pt centre and subsequent release and tautomerization of the modified NHP ligand to give

11; coordination of excess PPh₃ in solution either prior to, or after this release, would generate the hydride, **10**. Scheme 5(b) – Nucleophilic attack of H₂O at the Pt centre and subsequent deprotonation of coordinated water by NHP-turned-phosphide. The resultant Pt(II)-hydroxide may then decompose by either or both of two reductive elimination pathways (both analogous to that determined by Alper⁹⁹ for the oxidation of phosphines by Pd/OH⁻) to generate either O=PPh₃ and an analog of **10** that incorporates a secondary phosphine derived from the NHP, and/or to generate **10** and **11**. Although the formation of O=PPh₃ is favoured statistically by a 2:1 margin in route (b), we never observe it, nor do we see by NMR spectroscopy any metallic species other than **10** that incorporate phosphine and hydride.



Scheme 5. Proposed mechanisms for the hydrolysis of **1**.

The calculated natural atomic orbital charge distribution¹⁰⁰ in **1** (+ 1.09 for P, + 0.03 for Pt) also implicates the more cationic NHP phosphorus atom as the likely site for

nucleophilic attack by water. In addition, the total energies calculated for the P–OH/Pt–H and Pt–OH/P–H bonded intermediates in Scheme 5 indicate strong energetic preference for pathway (a): the initial attack of H₂O at P leads to a structure that is approximately 90 kJ mol⁻¹ more stable than the alternative platinum hydroxide. We therefore conclude that route (a) is the more reasonable pathway. This mechanism is further supported by calculated LUMO of **1**, which is localized predominantly on the NHP P-atom, with smaller contributions from the metal and N-atoms (Figure 4), and by the analogous reactivity of Group 6 metal–NHP complexes, which undergo nucleophilic attack by Me⁻ and EtO⁻ at the NHP, although dissociation of the resultant phosphine is not observed in these cases.¹⁰¹

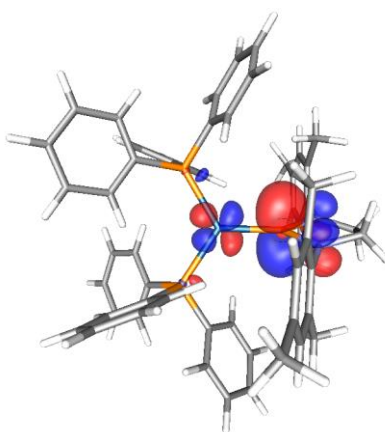
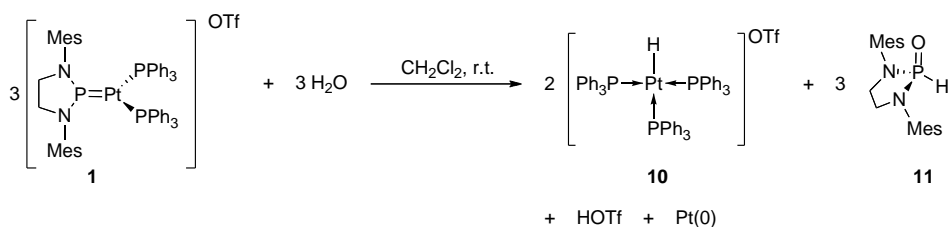


Figure 4. Calculated representation of the LUMO of **1** showing localization predominantly at the NHP P-atom. The metal coordination plane is approximately parallel to the page, and that of the NHP ligand is perpendicular to it.

In both routes (a) and (b), an additional molar equivalent of PPh₃ is necessary for formation of the observed products. In crude reaction mixtures towards the preparation of **1** (Scheme 4), we never observe deposition of Pt black, presumably owing to the presence

of excess PPh₃ from the Pt(PPh₃)₄ starting material in these systems. However, deliberate addition of H₂O to concentrated CH₂Cl₂ solutions containing pure, isolated samples of **1** gives the expected hydrolysis products **10** and **11**, and Pt black because of the stoichiometric deficiency of PPh₃ in these reactions (Scheme 6). No intermediates *en route* to the bulk metal are detected.

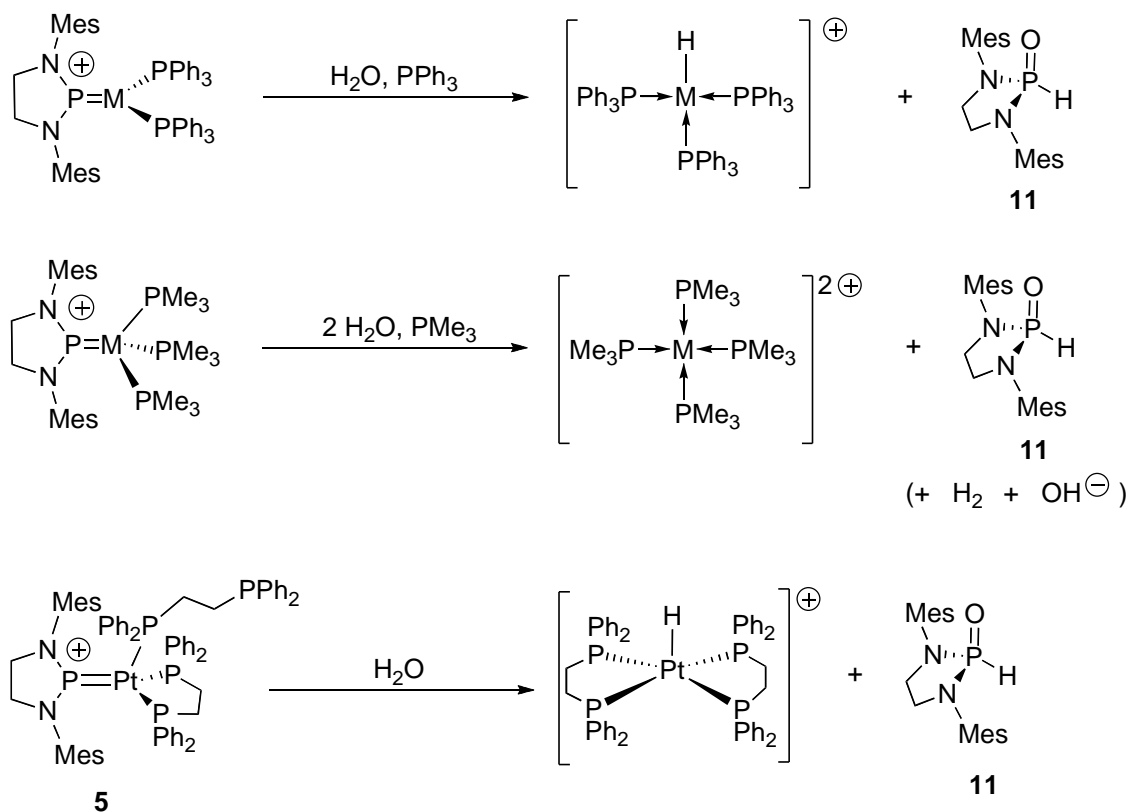


Scheme 6. Hydrolysis of isolated **1**.

The phosphine-containing hydrolysis product depends on the M–NHP starting material. Thus, the expected hydride, [HPt(PMe₃)₃]OTf¹⁰² does not form as the final product when **3** is hydrolyzed; instead, we observe the known homoleptic complex, [Pt(PMe₃)₄]OTf₂^{103,104} (Scheme 7). Presumably, the predicted cation [HPt(PMe₃)₃]⁺ is formed initially, but due to the greater Lewis basicity of PMe₃ relative to PPh₃ it is much more hydridic than **10** and very easily protonated by adventitious H₂O; the resultant coordinatively unsaturated [Pt(PMe₃)₃]²⁺ is then trapped by PMe₃ to give the final product.

Hydrolysis of **5** gives the five-coordinate platinum hydride, [PtH(dppe-κ²P)₂]OTf. A characteristic pentet (with Pt satellites) is observed in the high field region of the ¹H NMR spectrum of this species (δ -10.6, ¹J_{HPt} = 645 Hz, ²J_{HP} = 32 Hz), which unambiguously indicates the presence of a hydride coupled to four equivalent phosphines

and platinum. The $^{31}\text{P}\{^1\text{H}\}$ spectrum (δ 22.2, $^2J_{\text{HP}} = 22$ Hz, $^1J_{\text{PPt}} = 2344$ Hz)¹⁰⁵ is very similar to that of the known compound $[\text{PtH}(\text{dppe}-\kappa^2\text{P})_2]\text{PF}_6$ ¹⁰⁶ and analogous to that of the Pd complex which has been made previously from $[\text{Pd}(\text{dppe}-\kappa^2\text{P})_2]^{2+}$.¹⁰⁷



Scheme 7. Overall hydrolysis reactions of **1–5** in CH_2Cl_2 or CDCl_3 solution at r.t. All anions not shown are TfO^- .

Conclusions

Taken together, metrical parameters, computational results, and spectroscopic and reactivity data collectively support the interpretation that the most appropriate representation of **1** (and **2**) is that which shows an $\text{M}=\text{P}$ double bond and a formal

positive charge residing on the NHP phosphorus, *i.e.*, the phospho-Fischer carbene **D**, which is formally equivalent to **E** (Chart 4), albeit with diminished and augmented σ - and π -interactions, respectively, when compared to traditional carbon-based systems. This representation of the Group 10 metal(0) compounds is warranted also on the grounds of direct analogy to the characteristics generally attributed to Fischer carbenes,¹⁰⁸ and highlights the “diagonal relationship”¹⁸ between C and P: Fischer carbenes are derived from singlet $:\text{CR}_2$, contain an electrophilic carbene centre, have π -donor groups adjacent to the carbene centre, are typically associated with late metals in low oxidation states, and are found in conjunction with π -accepting ancillary ligands. We note also that Fischer carbenes are recognized as two-electron donors in both the covalent and ionic counting schemes, and do not change the formal oxidation state of the metal. We attribute these same characteristics to NHP complexes of Pt(0) and Pd(0).

Despite advances in synthesis, the onward reactivity of late metal-NHP complexes is all but unknown, and our initial investigations into substitution and hydrolysis reactions described herein will be followed by catalytic studies. The unique sterically encumbered and π -acidic character of NHP ligands holds great potential for rich and exciting new chemistry, as does the “operational unsaturation”^{109,110} that lies in the possibility for trigonal planar to pyramidal isomerism.

Acknowledgements. We acknowledge financial support from the Natural Sciences and Engineering Research Council of Canada (NSERC), a Petro-Canada Young Innovator’s Award (to NDJ), the Academy of Finland (to HMT) and an Ontario Graduate Scholarship (to CAC).

Supporting Information Available: Calculated coordinates for **1-4** and **6-9**, and X-ray crystallographic data for **1** (CIF). This material is available free of charge via the Internet at <http://pubs.acs.org>.

References

- (1) Fischer, E. O.; Maasböl, A. *Angew. Chem. Int. Ed.* **1964**, *3*, 580.
- (2) Dötz, K. H.; Fischer, H.; Hofmann, P.; Kreissl, F. R.; Schubert, U.; Weiss, K. *Transition Metal Carbene Complexes*; VCH: Weinheim, **1983**.
- (3) Schrock, R. R. *J. Am. Chem. Soc.* **1974**, *96*, 6796.
- (4) Schrock, R. R. *Acc. Chem. Res.* **1979**, *12*, 98.
- (5) Nguyen, S. T.; Johnson, L. K.; Grubbs, R. H. *J. Am. Chem. Soc.* **1992**, *114*, 3974.
- (6) Arduengo III, A. J.; Harlow, R. L.; Kline, M. *J. Am. Chem. Soc.* **1991**, *113*, 361.
- (7) Lavallo, V.; Canac, Y.; Präsang, C.; Donnadiou, B.; Bertrand, G. *Angew. Chem. Int. Ed.* **2005**, *44*, 5705.
- (8) Dyker, C. A.; Lavallo, V.; Donnadiou, B.; Bertrand, G. *Angew. Chem. Int. Ed.* **2008**, *47*, 3206.
- (9) Aldridge, S.; Coombs, D. L. *Coord. Chem. Rev.* **2004**, *248*, 535.
- (10) Irvine, G. J.; Lesley, M. J. G.; Marder, T. B.; Norman, N. C.; Rice, C. R.; Robins, E. G.; Roper, W. R.; Whittell, G. R.; Wright, L. J. *Chem. Rev.* **1998**, *98*, 2685.
- (11) Okazaki, M.; Tobita, H.; Ogino, H. *Dalton Trans.* **2003**, 493.
- (12) Waterman, R.; Hayes, P. G.; Tilley, T. D. *Acc. Chem. Res.* **2007**, *40*, 712.
- (13) Gudat, D. *Coord. Chem. Rev.* **1997**, *163*, 71.
- (14) Nakazawa, H. *J. Organomet. Chem.* **2000**, *611*, 349.

- (15) Nakazawa, H. In *Adv. Organomet. Chem.*; West, R. H., A.F., Ed.; Academic Press: Amsterdam, The Netherlands, **2004**; Vol. 50, p 107.
- (16) Cowley, A. H.; Kemp, R. A. *Chem. Rev.* **1985**, *85*, 367.
- (17) Sanchez, M.; Mazières, M.-R.; Lamandé, L.; Wolf, R. *Phosphorus Compounds with Coordination Number 2: Phosphenium Cations*; Thieme: Stuttgart, Germany, **1990**.
- (18) Dillon, K. B.; Mathey, F.; Nixon, J. F. *Phosphorus: The Carbon Copy: From Organophosphorus to Phospha-organic Chemistry*; John Wiley: Chichester, England, **1998**.
- (19) Tuononen, H. M.; Roesler, R.; Dutton, J. L.; Ragogna, P. J. *Inorg. Chem.* **2007**, *46*, 10693.
- (20) Spinney, H. A.; Yap, G. P. A.; Korobkov, I.; DiLabio, G.; Richeson, D. S. *Organometallics* **2006**, *25*, 3541.
- (21) Arduengo III, A. J. *Acc. Chem. Res.* **1999**, *32*, 913.
- (22) Bourissou, D.; Guerret, O.; Gabbai, F. P.; Bertrand, G. *Chem. Rev.* **2000**, *100*, 39.
- (23) Herrmann, W. A.; Köcher, C. *Angew. Chem. Int. Ed. Engl.* **1997**, *36*, 2162.
- (24) Gudat, D.; Haghverdi, A.; Hupfer, H.; Nieger, M. *Chem. Eur. J.* **2000**, *6*, 3414.
- (25) Montemayor, R. G.; Sauer, D. T.; Fleming, S.; Bennett, D. W.; Thomas, M. G.; Parry, R. W. *J. Am. Chem. Soc.* **1978**, *100*, 2231.
- (26) Nakazawa, H.; Yamaguchi, Y.; Miyoshi, K. *J. Organomet. Chem.* **1994**, *465*, 193.
- (27) Yamaguchi, Y.; Nakazawa, H.; Itoh, T.; Miyoshi, K. *Bull. Chem. Soc. Jpn.* **1996**, *69*, 983.
- (28) Gudat, D.; Haghverdi, A.; Nieger, M. *J. Organomet. Chem.* **2001**, *617-618*, 383.
- (29) Nakazawa, H.; Miyoshi, Y.; Katayama, T.; Mizuta, T.; Miyoshi, K.; Tsuchida, N.; Ono, A.; Takano, K. *Organometallics* **2006**, *25*, 5913.

- (30) Nakazawa, H.; Kishishita, M.; Nakamoto, T.; Nakamura, N.; Ishiyama, T.; Miyoshi, K. *Chem. Lett.* **2000**, 230.
- (31) Kawamura, K.; Nakazawa, H.; Miyoshi, K. *Organometallics* **1999**, *18*, 4785.
- (32) Abrams, M. B.; Scott, B. L.; Baker, R. T. *Organometallics* **2000**, *19*, 4944.
- (33) Burck, S.; Daniels, J.; Gans-Eichler, T.; Gudat, D.; Nättinen, K.; Nieger, M. Z. *Anorg. Allg. Chem.* **2005**, *631*, 1403.
- (34) Snow, S. S.; Jiang, D. X.; Parry, R. W. *Inorg. Chem.* **1987**, *26*, 1629.
- (35) Oberdörfer, R.; Nieger, M.; Niecke, E. *Chem. Ber.* **1994**, *127*, 2397.
- (36) Hardman, N. J.; Abrams, M. B.; Pribisko, M. A.; Gilbert, T. M.; Martin, R. L.; Kubas, G. J.; Baker, R. T. *Angew. Chem. Int. Ed. Engl.* **2004**, *43*, 1955.
- (37) Collman, J. P.; Segedus, L. S.; Norton, J. R.; Finke, R. G. *Principles and Applications of Organotransition Metal Chemistry*; University Science Books: Mill Valley, California, **1987**.
- (38) Hutchins, L. D.; Paine, R. T.; Campana, C. F. *J. Am. Chem. Soc.* **1980**, *102*, 4521.
- (39) Hutchins, L. D.; Duesler, E. N.; Paine, R. T. *Organometallics* **1982**, *1*, 1254.
- (40) Parkin, G. *Organometallics* **2006**, *25*, 4744.
- (41) Caputo, C. A.; Price, J. T.; Jennings, M. C.; McDonald, R.; Jones, N. D. *Dalton Trans.* **2008**, 3461.
- (42) Bernasconi, C. F.; Leyes, A. E. *J. Chem. Soc., Perkin Trans. 2* **1997**, 1641.
- (43) Zoloff Michoff, M. E.; de Rossi, R. H.; Granados, A. M. *J. Org. Chem.* **2006**, *71*, 2395.
- (44) Bernasconi, C. F.; Flores, F. X.; Kittredge, K. W. *J. Am. Chem. Soc.* **1997**, *119*, 2103.

- (45) Ugo, R.; Cariati, F.; La Monica, G. In *Reagents for Transition Metal Complex and Organometallic Syntheses and Organometallic Syntheses*; Angelici, R. J., Ed.; John Wiley & Sons Inc.: New York, **1990**; Vol. 28, p 123.
- (46) Coulson, D. R. In *Reagents for Transition Metal Complex and Organometallic Syntheses*; Angelici, R. J., Ed.; John Wiley & Sons Inc.: New York, **1990**; Vol. 28, p 107.
- (47) Perdew, J. P.; Burke, K.; Ernzerhof, M. *Phys. Rev. Lett.* **1996**, 77, 3865.
- (48) Perdew, J. P.; Burke, K.; Ernzerhof, M. *Phys. Rev. Lett.* **1997**, 78, 1396.
- (49) Perdew, J. P.; Ernzerhof, M.; Burke, K. *J. Chem. Phys.* **1996**, 105, 9982.
- (50) Schäfer, A.; Huber, C.; Ahlrichs, R. *J. Chem. Phys.* **1994**, 100, 5829.
- (51) Eichkorn, K.; Weigend, F.; Treutler, O.; Ahlrichs, R. *Theor. Chem. Acc.* **1997**, 97, 119.
- (52) Andrae, D.; Haeussermann, U.; Dolg, M.; Stoll, H.; Preuss, H. *Theor. Chem. Acc.* **1990**, 77, 123.
- (53) TURBOMOLE In *Program Package for ab initio Electronic Structure Calculations*; Version 5.10 ed.; Theoretical Chemistry Group, University of Karlsruhe: Karlsruhe, Germany, **2008**.
- (54) Ahlrichs, R.; Bär, M.; Häser, M.; Horn, H.; Kölmel, C. *Chem. Phys. Lett.* **1989**, 162, 165.
- (55) ADF2007.01 In *Theoretical Chemistry Program*; SCM, V. U., Ed. Amsterdam, Netherlands, **2007**.
- (56) Morokuma, K. *J. Chem. Phys.* **1971**, 55, 1236.
- (57) Kitaura, K.; Morokuma, K. *Int. J. Quantum Chem.* **1976**, 10, 325.
- (58) Ziegler, T.; Rauk, A. *Theoret. Chim. Acta* **1977**, 46, 1.
- (59) van Lenthe, E.; Baerends, E. J. *J. Comp. Chem.* **2003**, 24, 1142.

- (60) Chong, D. P.; van Lenthe, E.; van Gisbergen, S.; Baerends, E. J. *J. Comp. Chem.* **2004**, *25*, 1030.
- (61) van Lenthe, E.; Baerends, E. J.; Snijders, J. G. *J. Chem. Phys.* **1993**, *99*, 4597.
- (62) van Lenthe, E.; Baerends, E. J.; Snijders, J. G. *J. Chem. Phys.* **1994**, *101*, 9783.
- (63) van Lenthe, E.; Ehlers, A. E.; Baerends, E. J. *J. Chem. Phys.* **1999**, *110*, 8943.
- (64) Laaksonen, L. *J. Mol. Graph.* **1992**, *10*, 33.
- (65) Bergman, D. L.; Laaksonen, L.; Laaksonen, A. *J. Mol. Graph. Model.* **1997**, *15*, 301.
- (66) Ackermann, L.; Born, R. *Angew. Chem. Int. Ed.* **2005**, *44*, 2444.
- (67) Sakakibara, K.; Yamashita, M.; Nozaki, K. *Tetrahedron Lett.* **2005**, *46*, 959.
- (68) Scriban, C.; Glueck, D. S.; DiPasquale, A. G.; Rheingold, A. L. *Organometallics* **2006**, *25*, 5435.
- (69) Kourkine, I. V.; Chapman, M. B.; Glueck, D. S.; Eichele, K.; Wasylishen, R. E.; Yap, G. P. A.; Liable-Sands, L. M.; Rheingold, A. L. *Inorg. Chem.* **1996**, *35*, 1478.
- (70) Orpen, A. G.; Brammer, L.; Allen, F. H.; Kennard, O.; Watson, D. G.; Taylor, R. *J. Chem. Soc., Dalton Trans.* **1989**, S1.
- (71) Tolman, C. A. *Chem. Rev.* **1977**, *77*, 313.
- (72) Hu, X.; Tang, Y.; Gantzel, P.; Meyer, K. *Organometallics* **2003**, *22*, 612.
- (73) Hu, X.; Castro-Rodrigues, I.; Olsen, K.; Meyer, K. *Organometallics* **2004**, *23*, 755.
- (74) Nemcsok, D.; Wichmann, K.; Frenking, G. *Organometallics* **2004**, *23*, 3640.
- (75) Frenking, G.; Solà, M.; Vyboishchikov, S. F. *J. Organomet. Chem.* **2005**, *690*, 6178.

- (76) Jacobsen, H.; Correa, A.; Costabile, C.; Cavallo, L. *J. Organomet. Chem.* **2006**, *691*, 4350.
- (77) Boehme, C.; Frenking, G. *Organometallics* **1998**, *17*, 5801.
- (78) Jacobsen, H.; Correa, A.; Poater, A.; Costabile, C.; Cavallo, L. *Coord. Chem. Rev.* **2008**, doi:10.1016/j.ccr.2008.06.006.
- (79) Gudat, D. *Eur. J. Inorg. Chem.* **1998**, 1087.
- (80) Takano, K.; Tsumura, H.; Nakazawa, H.; Kurakata, M.; Hirano, T. *Organometallics* **2000**, *19*, 3323.
- (81) Bickelhaupt, F. M.; Baerends, E. J. *Rev. Comput. Chem.*; Wiley-VCH: New York, **2000**; Vol. 15.
- (82) The total bonding energy calculated in this manner is, however, not the negative of bond dissociation enthalpy as the former quantity does not take into account the fragment relaxation and reorganization processes inherent in real bonding schemes.
- (83) Lein, M.; Szabó, A.; Kovács, A.; Frenking, G. *Faraday Discuss.* **2003**, *124*, 365.
- (84) Cases, M.; Frenking, G.; Duran, M.; Solà, M. *Organometallics* **2002**, *21*, 4182.
- (85) Gelloz-Berthon, G.; Buisine, O.; Brière, J.-F.; Michaud, G.; Stérin, S.; Mignani, G.; Tinant, B.; Declercq, J.-P.; Chapon, D.; Markó, I. E. *J. Organomet. Chem.* **2005**, *690*, 6156.
- (86) Arnold, P. L.; Cloke, F. G. N.; Geldbach, T.; Hitchcock, P. B. *Organometallics* **1999**, *18*, 3228.
- (87) Caddick, S.; Cloke, F. G. N.; Hitchcock, P. B.; Leonard, J.; Lewis, A. K. d. K.; McKerrecher, D.; Titcomb, L. R. *Organometallics* **2002**, *21*, 4318.

- (88) Jackstell, R.; Harkal, S.; Jiao, H.; Spannenberg, A.; Borgmann, C.; Röttger, D.; Nierlich, F.; Elliot, M.; Niven, S.; Cavell, K. J.; Navarro, O.; Viciu, M. S.; Nolan, S. P.; Beller, M. *Chem. Eur. J.* **2004**, *10*, 3891.
- (89) Clement, N. D.; Cavell, K. J.; Ooi, L. *Organometallics* **2006**, *25*, 4155.
- (90) Fantasia, S.; Nolan, S. P. *Chem. Eur. J.* **2008**, *14*, 6987.
- (91) We note that this is only a rough division as the proper definition of symmetry implies the presence of a mirror plane and not a C_2 axis. Therefore, some of the orbitals, which should be classified as symmetric transfer as the b and a representations of the C_2 point group, respectively. Consequently, the reported contributions to bonding are slightly under- and overestimated. However, the error is expected to be only minor as the metal-phosphorus bond lies on the C_2 axis.
- (92) Xile, H.; Yongjun, T.; Gantzel, P.; Meyer, K. *Organometallics* **2003**, *22*, 612.
- (93) Dewar, M. J. S. *Bull. Soc. Chim. Fr.* **1951**, *18*, C79.
- (94) Chatt, J.; Duncanson, L. A. *J. Chem. Soc.* **1953**, 2939.
- (95) Thomas, K.; Dumler, J. T.; Renoe, B. W.; Nyman, C. J.; Roundhill, D. M. *Inorg. Chem.* **1972**, *11*, 1795.
- (96) Chinakov, V. D.; Il'inich, G. N.; Zudin, V. N.; Likholobov, V. A.; Nekipelov, V. M. *J. Organomet. Chem.* **1989**, *366*, 421.
- (97) Goel, R. G.; Srivastava, R. C. *J. Organomet. Chem.* **1983**, *244*, 303.
- (98) Caputo, R. E.; Mak, D. K.; Willett, R. D.; Roundhill, S. G. N.; Roundhill, D. M. *Acta Cryst.* **1977**, *B33*, 215.
- (99) Grushin, V. V.; Alper, H. *Organometallics* **1993**, *12*, 1890.
- (100) Reed, A. E.; Weinstock, R. B.; Weinhold, F. *J. Chem. Phys.* **1985**, *83*, 735.
- (101) Nakazawa, H.; Ohta, M.; Miyoshi, K.; Yoneda, H. *Organometallics* **1989**, *8*, 638.

- (102) Packett, D. L.; Syed, A.; Trogler, W. C. *Organometallics* **1988**, *7*, 159.
- (103) Hahn, F. E.; Langenhahn, V.; Lügger, T.; Pape, T.; Le Van, D. *Angew. Chem. Int. Ed.* **2005**, *44*, 3759.
- (104) Kozelka, J.; Lüthi, H.-P.; Dubler, E.; Kunz, R. W. *Inorg. Chim. Acta.* **1984**, *86*, 155.
- (105) The ^1H decoupler was on for this ^{31}P experiment, however it was unable to fully decouple the hydride proton. As a result, a doublet was still visible, but the $^1J_{\text{HP}}$ value was slightly smaller than that observed in the ^1H NMR spectrum.
- (106) Berning, D. E.; Noll, B. C.; DuBois, D. L. *J. Am. Chem. Soc.* **1999**, *121*, 1432.
- (107) Aresta, M.; Quaranta, E. *J. Organomet. Chem.* **2002**, *662*, 112.
- (108) Crabtree, R. H. *The Organometallic Chemistry of the Transition Metals*; John Wiley & Sons, Inc.: New Haven, Connecticut, **2001**.
- (109) Johnson, T. J.; Huffman, J. C.; Caulton, K. G. *J. Am. Chem. Soc.* **1992**, *114*, 2725.
- (110) Johnson, T. J.; Coan, P. S.; Caulton, K. G. *Inorg. Chem.* **1993**, *32*, 4594.